1994A&A...283..144F

Astron. Astrophys. 283, 144–154 (1994)

ASTRONOMY AND ASTROPHYSICS

OB-type binaries: models versus observations

J. Figueiredo[1,*], and J.P. De Greve[1,], and R.W. Hilditch[2]**

[1] Astrophysical Institute, VUB, Pleinlaan 2, B-1050 Brussels, Belgium
[2] Department of Physics and Astronomy, University of St. Andrews, North Haugh, St. Andrews, Fife KY16 9SS, Scotland

Received March 12, accepted August 10, 1993

Abstract. Recently published models on close binary evolution for massive stars ($M > 5M_{\odot}$) are compared to a set of detached and semidetached OB binaries.

For the majority of the detached systems, we find good correspondence between theoretical and observed characteristics for stars with masses between $4.5M_{\odot}$ and $17M_{\odot}$.

We explore the origin of semidetached systems, and discuss anomalies between models and observed characteristics. An initial mass ratio of around 0.6 seems to be preferred for this group.

Finally, we briefly examine a number of massive (marginal) contact systems. The latter systems all seem to evolve according to case A of mass transfer.

Key words: stars: evolution – binaries: close – stars: early-type – stars: fundamental parameters

1. Introduction

Comparisons between theoretical stellar models and observed characteristics of stars have always been a fundamental tool for testing the validity of the models. The largest uncertainty in the comparison is the chemical composition (Andersen 1991). It influences severely the models through the absorption coefficients and it remains very uncertain (or even quantitatively unknown) in the observational analysis.

Detached binaries offer a very interesting opportunity to test the models, since their masses, radii, effective temperatures and luminosities of the components may be known with some accuracy (Andersen 1991).

Recently models for massive single stars, including overshooting of the convective core and mass loss by stellar wind, reached a satisfying agreement with present observations (Maeder & Meynet 1987; Schaller et al. 1992), though the uncertainties on the amount of overshooting (Brocato & Castellani 1991; Zahn 1991) and the mass loss rate remain.

Send offprint requests to: J.P. De Greve
* Also Centro de Astrofísica da Universidade do Porto
** Research Director, NFWO, Belgium

In addition to the models for single stars de Loore & De Greve (1992) published a series of models for massive close binaries, with comparable input physics (see also De Greve & de Loore 1992). A similar set for the lower masses, without stellar wind mass loss, was published by De Greve (1993).

For the observational data, Hilditch & Bell (1987, further referred as HB87) published a compilation of characteristics of 31 binary systems in the range O-B5, with comparable quality to those in Popper's (1980) review. The quality of these data does not achieve the stringent conditions imposed by Andersen (1991) in his review on detached binary stars. However for the most massive detached systems, and for the semidetached and contact systems, those cited in HB87 represented the best available data at that time. In the intervening six years significant improvements have been brought to the observational results for some systems, and results for new systems have also been published. It seems pertinent therefore to re-examine the comparison between observational data and the new theoretical models incorporating mass loss, convective overshooting, and the fraction of mass transferred between the components in binary stars.

In this paper we confront the theoretical models with the observations. Based upon the satisfactory agreement, we then compare the interacting (semidetached) systems to study the influence of the foregoing interacting evolution.

The choice of both theoretical models and observed systems is led by the need for coherence within each set of data.

In Sect. 2, we discuss briefly the characteristics of the observational data and theoretical models. The comparison is made in Sect. 3 for the detached systems and in Sect. 4 for the semidetached systems. In Sect. 5 we treat the contact systems and in Sect. 6 we discuss the results and draw some conclusions. In this paper we will follow the observer's approach, e.g. in referring to component quantities subscript 1 refers to the hotter star, subscript 2 to the cooler star. In order to avoid confusion between the observer's language and the theoretician's description we will additionally use gainer and loser as component indicators, instead of primary and secondary.

© European Southern Observatory • Provided by the NASA Astrophysics Data System

1994A&A...283..144F

2. Observations and theoretical results

2.1. Observations

For the observed systems, we use the characteristics of the systems given by HB87. Their compilation contains 16 detached systems, 7 contact systems (marginal contact for most of them), and 8 semidetached systems. The characteristics are masses, radii, effective temperatures and luminosities. Since that publication a number of these systems have been re-analyzed with additional observational data and new ones have been studied. These revisions and additions are compiled in Table 1, which is complete upto February 1993. It was interesting, though not surprising, that most of the new data considerably improved the results of the earlier comparison between the original HB87 data and the theoretical models. This is especially true for the systems discussed in the next paragraph.

EM Car and NY Cep are new detached systems. Except for U Oph, for which the changes in the two revised solutions remain small for all the parameters, the changes are most severe for the masses, especially for the systems V382 Cyg (an increase of 21%) and AH Cep (a decrease of 15%). The largest changes in luminosity occur in V478 Cyg (detached; a decrease for both components), AH Cep (detached; lower mass component decreased) and DM Per (semidetached; increase of the bright component).

The choice of short period systems, made by HB87 in their sample, causes some bias among the semidetached systems (as was also noticed by these authors). Normally one expects semidetached systems to have a well reversed mass ratio and a substantial radius excess of the subgiant over the bright star (in case of a large period). In the present sample only 3 out of 8 systems show this excess: TT Aur, V356 Sgr and DM Per. V356 Sgr is the only system with a large excess ($R_1/R_2 = 0.43$, with R_1 the radius of the hotter star and R_2 the cooler subgiant radius), but it is also the only system in the sample with a large period. For DM Per, with a period of 2.7 d and a mass ratio $q = M_1/M_2 = 4$, the radii are nearly equal ($R_1/R_2 = 0.95$, as for TT Aur (0.93)). The same prevalence may also explain the presence of 4 systems with mass ratio smaller than 2, because the chance of observing short period systems earlier in the mass transfer

Table 1. O-B5 binary systems with updated parameters compared to the compilation of HB87. The table lists the system name, primary (p) and secondary (s) component, mass (in $M_\odot$), error on mass (in $M_\odot$), radius (in $R_\odot$), error on radius (in $R_\odot$), logarithm of effective temperature, error on temperature (in dex), logarithm of the luminosity, error on the luminosity (in dex), references

System		Mass	Err.	Radius	Err.	Log T	Err.	Log L	Err.	Ref.
EM Car	p	22.890	0.320	9.340	0.170	4.531	0.026	5.020	0.100	1, 2
	s	21.430	0.330	8.330	0.140	4.531	0.026	4.920	1.100	
V478 Cyg	p	16.670	0.450	7.423	0.079	4.484	0.015	4.630	0.060	3, 2
	s	16.310	0.350	7.423	0.079	4.485	0.015	4.630	0.060	
CW Cep	p	13.520	0.390	5.685	0.130	4.452	0.015	4.270	0.060	3, 4, 2
	s	12.080	0.290	5.177	0.129	4.442	0.016	4.150	0.070	
U Oph	p	5.198	0.113	3.438	0.044	4.220	0.020	2.910	0.080	2, 3
	s	4.683	0.090	3.005	0.055	4.199	0.020	2.700	0.080	
U Oph	p	4.930	0.050	3.290	0.060	4.228	0.037	2.880	0.160	5
	s	4.560	0.040	3.010	0.050	4.204	0.039	2.710	0.160	
V382 Cyg	p	32.600	1.800	8.800	0.600	4.575	0.020	5.140	0.060	3
	s	22.900	1.300	7.400	0.600	4.565	0.020	4.950	0.070	
AH Cep	p	15.400	0.200	6.380	0.110	4.476	0.014	4.448	0.140	6, 7
	s	13.600	0.200	5.860	0.130	4.456	0.015	4.296	0.160	
V453 Cyg	p	13.900	0.700	8.500	0.300	4.470	0.015	4.690	0.030	3
	s	10.700	0.600	5.300	0.150	4.450	0.025	4.180	0.020	
TT Aur	p	8.100	0.400	3.900	0.100	4.395	0.020	3.710	0.030	3, 9, 10
	s	5.400	0.300	4.200	0.100	4.255	0.020	3.210	0.030	
DM Per	p	7.310	0.140	4.500	0.090	4.255	0.020	3.280	0.100	11
	s	2.070	0.06	4.750	0.090	3.924	0.010	2.000	0.160	
NY Cep	p	13.000	1.000	6.800	0.700	4.455	0.015	4.450	0.300	12
	s	9.000	1.000	5.400	0.500	4.364	0.018	3.860	0.200	
AG Per	p	5.400	0.150	3.170	0.150	4.425	0.030	2.900	0.040	3
	s	4.950	0.150	2.870	0.150	4.210	0.030	2.170	0.040	

References : 1. Andersen & Clausen (1989); 2 Andersen (1991); 3. Popper & Hill (1991); 4. Clausen & Gimenez (1991); 5. Holmgren & Hill (1991); 6. Holmgren et al. (1990); 7. Bell et al. (1986); 8. Polidan (1989); 9. Bell et al. (1987); 10. Wachman et al. (1986); 11. Hilditch et al. (1992); 12. Holmgren et al. (1990).

© European Southern Observatory • Provided by the NASA Astrophysics Data System

1994A&A...283..144F

is larger. Nevertheless, all systems have a mass ratio well beyond 1. We may therefore assume that they are all ending the fast phase of mass transfer or have evolved further into the slow phase.

2.2. Models

From the theoretical side we use the series of evolutionary sequences for binary stars in the mass range 9–40$M_\odot$ (de Loore & De Greve 1992) and the corresponding analysis of these data (De Greve & de Loore 1992). The models are calculated with the same algorithms for the calculation of the overshooting and the stellar wind mass loss as the single star models of Schaller et al. (1992). The opacities used are those from the Los Alamos Opacity Library. Since then, new opacities have been published (Rogers & Iglesias 1992), but it was shown by De Greve (1993) that these do not affect the mass values at the end of the mass transfer. Mass transfer is calculated according to the early case B mode (onset after core hydrogen burning; Kippenhahn & Weigert 1966), assuming that 50% of the matter is lost from the system. These series were supplemented by the series for masses between 3$M_\odot$ and 8$M_\odot$ (De Greve 1993) to account for the lower masses in the observational data set. The latter calculations are similar to those of de Loore & De Greve, except that stellar wind mass loss is neglected.

3. Detached systems

The components of all the detached systems were located in the Hertzsprung–Russell diagram, with the error bars as given by HB87. Their positions were compared to two (sometimes three) neighbouring evolutionary main sequence tracks from the set of models. The masses deduced from the models are compared to the observed mass. As an example, Fig. 1 shows the location of the components of DI Her, with an excellent agreement between models and observations. Figures 2 and 3 show the location of the components of V380 Cyg and of α Vir as typical examples where the agreement was poor, the deviations in masses being of the order of 35% (V380 Cyg), resp. 10–20% (α Vir, but in opposite direction for the two components). If we adopt the observed masses of V380 Cyg, then both components are overluminous, especially the primary (the corresponding theoretical luminosity of a 14.3$M_\odot$ star at the end of the main sequence is $\log L/L_\odot \sim 4.5$, instead of the observed 4.98 ± 0.08). For the components of α Vir the situation is different. The bright component is overluminous for its mass, while the less massive secondary is underluminous.

Table 2 summarizes the results for all the detached systems, obtained through the comparison. The total sample contains 16 systems, but 31 stars (for BM Ori only the parameters of the hot component are known with enough

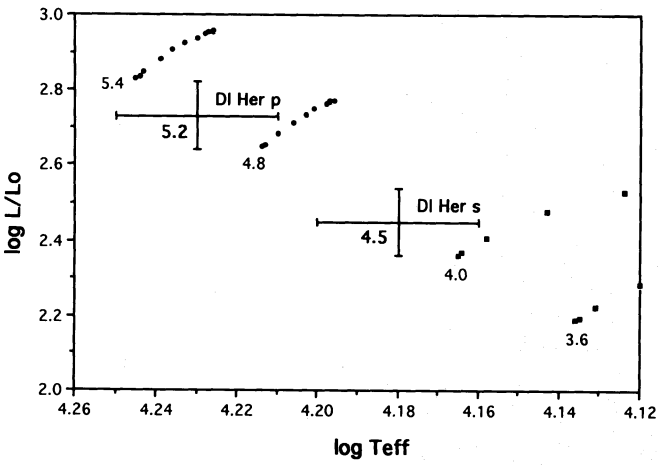

Fig. 1. HR diagram of the two components of DI Her (p: primary = gainer, s: secondary = loser) together with the evolutionary tracks (main sequence part). Numbers at the beginning of the tracks indicate the mass of the star, the bold numbers are the masses of the components (in $M_\odot$), as derived from observations

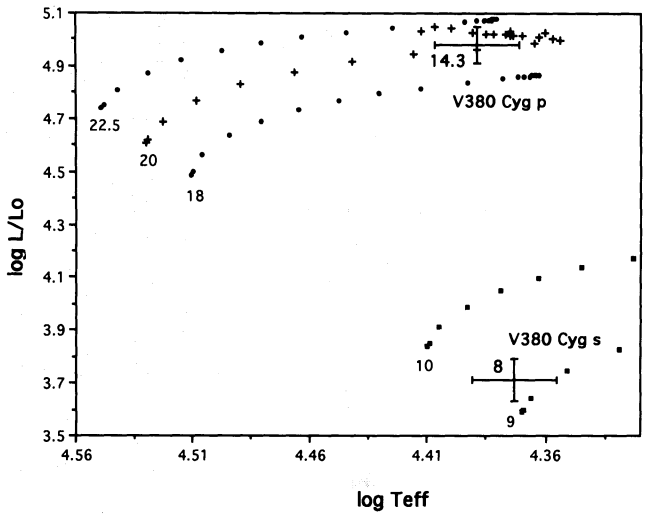

Fig. 2. The same as Fig. 1, but for the system V380 Cyg

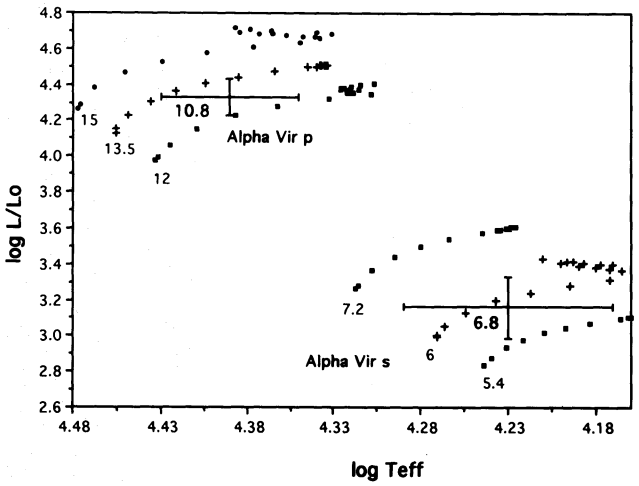

Fig. 3. The same as Fig. 1, but for the system Alpha Vir

© European Southern Observatory • Provided by the NASA Astrophysics Data System

1994A&A...283..144F

Table 2. Results of the comparison of the observed masses of the components of detached systems, with theoretical lower $M_{\text{th-down}}$ and upper limits $M_{\text{th-up}}$ derived from evolutionary tracks. Masses are in solar masses; diff. mean = $(M_{\text{th-up}} - M_{\text{th-down}})/2$-(observed) mass; diff. mean % = diff.mean/(observed) mass. The conclusion ok denotes an agreement better than 15%

System	Comp.	Mass	Err. (m)	$M_{\text{th-down}}$	$M_{\text{th-up}}$	Diff. mean	Diff. mean%	Concl.
AG Per	p	5.400	0.150	5.00	6.10	0.15	0.03	ok
AG Per	s	4.950	0.150	4.30	5.20	0.20	0.04	ok
AH Cep	p	15.400	0.200	14.56	17.56	0.66	0.04	ok
AH Cep	s	13.600	0.200	13.41	15.00	0.61	0.04	ok
Alpha Vir	p	10.789	1.292	11.50	14.30	2.11	0.20	Th. > Obs.
Alpha Vir	s	6.792	0.907	5.00	6.90	−0.84	−0.12	ok
BM Ori	p	5.902	0.081	5.70	7.20	0.55	0.09	ok
CV Vel	p	6.095	0.042	5.40	7.00	0.11	0.02	ok
CV Vel	s	5.998	0.041	5.50	7.00	0.25	0.04	ok
CW Cep	p	13.520	0.390	13.14	14.82	0.46	0.03	ok
CW Cep	s	12.080	0.290	12.01	13.90	0.88	0.07	ok
DI Her	p	5.152	0.095	4.70	5.40	−0.10	−0.02	ok
DI Her	s	4.519	0.062	4.00	4.60	−0.22	−0.05	ok
QX Car	p	9.268	0.128	9.10	9.50	0.03	0.00	ok
QX Car	s	8.472	0.117	8.30	9.00	0.18	0.02	ok
U Oph	p	5.164	0.095	4.93	5.63	0.11	0.02	ok
U Oph	s	4.603	0.064	4.45	5.05	0.15	0.03	ok
V1182 Aql	p	37.757	3.217	24.40	29.00	−11.06	−0.29	Th. < Obs.
V1182 Aql	s	13.490	0.994	12.10	14.80	−0.04	0.00	ok
V380 Cyg	p	14.289	0.529	19.00	22.50	6.46	0.45	Th. > Obs.
V380 Cyg	s	7.998	0.295	8.80	9.60	1.20	0.15	Th. > Obs.
V453 Cyg	p	13.900	0.700	17.58	18.52	4.15	0.30	Th. > Obs.
V453 Cyg	s	10.700	0.600	12.47	14.75	2.91	0.27	Th. > Obs.
V478 Cyg	p	16.670	0.450	16.57	18.83	1.03	0.06	ok
V478 Cyg	s	16.310	0.350	16.47	18.73	1.29	0.08	ok
V539 Ara	p	6.252	0.072	5.90	7.00	0.20	0.03	ok
V539 Ara	s	5.333	0.061	5.00	6.10	0.22	0.04	ok
V760 Sco	p	4.977	0.092	5.00	5.40	0.22	0.04	ok
V760 Sco	s	4.624	0.074	4.60	5.00	0.18	0.04	ok
Y Cyg	p	16.711	0.500	14.50	18.00	−0.46	−0.03	ok

accuracy – cf. Popper 1980). For 24 stars the deviation between the observed mass value and the theoretical one is less than 15%. Out of these, 23 have a deviation of less than 10%, and 18 even less than 5%. We discuss briefly the most anomalous systems.

V1182 Aql: The orbit solution is based on only 5 observations at the (double-lined) quadrature phases; hence masses must be regarded as preliminary.

V453 Cyg: Both the photometric data and the spectroscopic data are well defined and self-consistent. There is no evidence for systematic errors.

V380 Cyg: Although the cooler component is definitely seen in the cross-correlation functions (CCF) and consistent measurements could be made for radial velocity by Hill & Batten (1984), it remains the case that this star does not present a clearly resolved peak in the CCF. Accordingly, some uncertainty must remain over the velocity semi-amplitude derived for the cooler star. With an orbital period of 12.4 d, it is not surprising that the lightcurve is incomplete. The depths of the eclipses are small (0.12 and 0.09 mag) and hence determinations of the radii and of the orbital inclination will not be accomplished with the usual precision. Hill & Batten did however combine all the empirical knowledge of this system (rotational velocities, spectroscopic luminosity ratio, equivalent widths of selected lines, etc.) in deriving the final parameters for the system. The largest single uncertainty is probably the semi-amplitude of the velocity curve of the cool component which crucially affects the derived mass of the hot component. New spectroscopic observations are required.

α Vir: The spectroscopic observations of this system are at high resolution, but recorded on coarse-grained photographic plates. Oscilloscopic techniques were used for measurements of line position so that line-blending problems (Hilditch 1973; Andersen 1975, 1991; Popper & Hill 1991) ought not to be serious. Care was taken to account for the asymmetric profiles seen in some lines as a result of

© European Southern Observatory • Provided by the NASA Astrophysics Data System

1994A&A...283..144F

ß Cephei type pulsations, and the resultant velocity semi-amplitudes would seem to be well defined. By contrast, the total amplitude of the binary light curve (separate from that due to the ß Cephei phenomenon) is only 3% (Shobbrook et al. 1969) and is due to aspect changes of a tidally-distorted star. The orbital inclination is derived from interferometric observations so that the stellar radii are constrained by the amplitude of the light curve and the known luminosities and temperatures. New spectroscopic observations would be helpful.

4. Semidetached systems

Based on the satisfying agreement, obtained for the detached systems, we can examine the semidetached systems. Because of the more complex evolution, the goal is here twofold: finding inconsistencies between theory and observations, and deriving information on their earlier evolution (i.e. their origin). For the moment, we will assume that all the observed systems in the sample are indeed case B systems, and that the 50% mass loss from the system is a good approximation of reality.

4.1. Mass losing components (losers)

Because its radius is fixed by the period P and the condition being semidetached, and its effective temperature by the spectral type, we determine the initial mass of this component and the advance in the mass transfer process from the mass-luminosity diagram. This is shown in Fig. 4. As the systems are beyond mass ratio reversal and entering (or are already in) a slow phase of mass transfer, we assume that the luminosity of the loser is no longer decreasing (hence it is around L_{min} or in the luminosity increasing slow phase). The estimates for the initial masses, derived for two values of the initial mass ratio, are given in Table 3 (within $0.5M_{\odot}$). The values derived for $q_i = 0.6$ (q_i defined as M_{2i}/M_{1i}) are generally somewhat larger than $q_i = 0.9$, because the mass–luminosity curves are steeper for lower initial mass ratios (De Greve 1986). The systems Z Vul and DM Per are interesting because they have similar progenitor masses (for the loser), are in the same phase of mass transfer, and have comparable periods. The same holds for TT Aur and SX Aur. For $q_i = 0.9$, the more massive systems, AI Cru and V Pup (perhaps also TT Aur and SX Aur), are close to the minimum luminosity, whereas for $q_i = 0.6$, all systems are near or in the slow phase of mass transfer (strong photometric variabilities indicating the presence of circumstellar matter would favour the larger mass ratio).

4.2. The mass accreting component (gainer)

For the mass accreting component, we use the radius and the luminosity for the comparison. As pointed our by De Greve & Loore (1992) (see also De Greve 1993) gainers tend to deviate from normal main sequence stars, especially

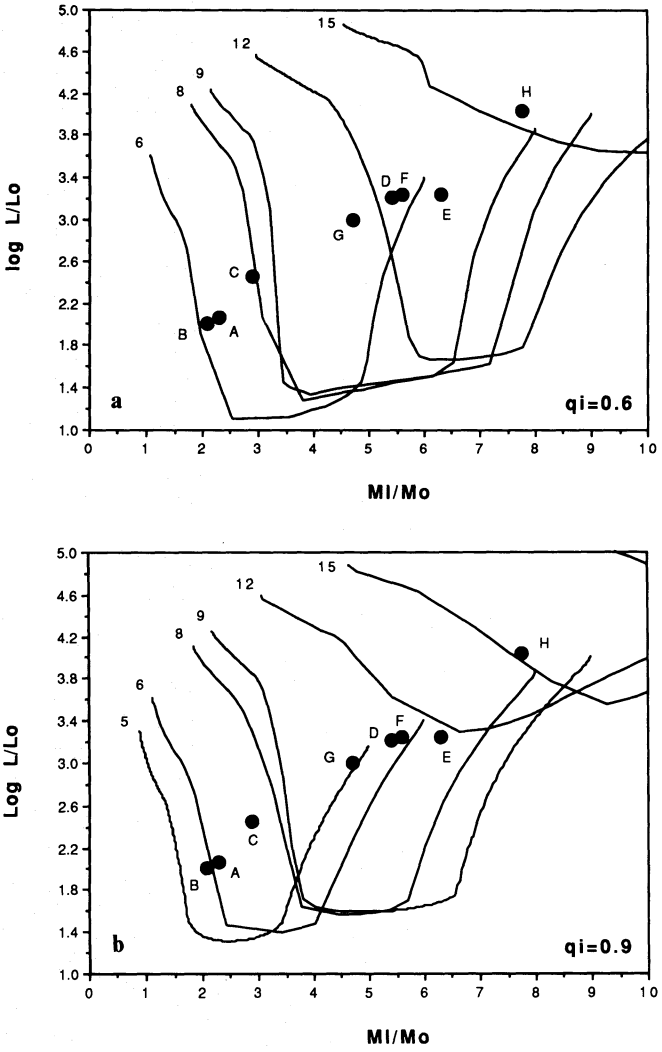

Fig. 4a and b. Mass–luminosity diagram with tracks of mass losing stars taken from De Greve (1993) and de Loore & De Greve (1992), together with the positions of the observed losers of semidetached systems (the characters refer to Table 3). The initial masses (in solar masses) corresponding to the evolutionary tracks for the mass losing component are indicated. The results for two initial mass ratios $q_i = 0.6$ (**a**) and $q_i = 0.9$ (**b**) are shown

around the phase of minimum luminosity of the loser. The radii and luminosities are larger than those of normal stars, as a result of the accretion of matter (Benson 1970; Kippenhahn & Hofmeister 1977; Flannery & Ulrich 1977; Packet & De Greve 1979; Packet 1988). However direct comparison is not possible, because we do not know the internal structure of the gainer (i.e. how far it is advanced in the core hydrogen burning stage). But from the analyses of De Greve & de Loore (1992) and De Greve (1993) we find that initial mass ratios 0.9 and 0.6 result in central hydrogen abundances for the gainers of typically 0.2–0.3 and 0.5–0.6 resp., once the system is beyond minimum luminosity. There is no clear mass ratio range corresponding to each of the two sets of central hydrogen values (the

© European Southern Observatory • Provided by the NASA Astrophysics Data System

1994A&A...283..144F

Table 3. Estimated initial masses for some semi-detached systems (all expressed in solar masses); l and g denote loser and gainer resp.. The first two columns give the initial mass of the loser for two different values of the initial mass ratio, as derived from the mass–luminosity diagram of the loser. The next four columns give the initial masses of gainer (and corresponding loser) as derived from mass–luminosity (L) and mass–radius (R) diagrams for $q_i = 0.6$. The two columns labeled $M_{l,obs}$ and $M_{g,obs}$ give the observed values of the loser and of the gainer. The last column gives the value of $\beta = \Delta M_g/\Delta M_l$ derived from the observed masses and the initial values for $q_i = 0.6$

		M_{li}/M_o	M_{li}/M_o	M_{gi}/M_o	M_{li}/M_o	M_{gi}/M_o	M_{li}/M_o	$M_{l,obs}$	$M_{g,obs}$	Beta
	System	$q_i = 0.9$	$q_i = 0.6$	0.6-L	L-curve	0.6-R	R-curve			
A	Z Vul	6	7	3.6	6	3.6	6	2.3	5.4	0.38
B	DM Per	6	6	4.2	7	4.8	8	2.1	7.3	0.64
C	U Her	7	8	4.8	8	4.8	8	2.9	7.6	0.55
D	TT Aur	11	12.5	5.1	8.5	5.1	8.5	5.4	8.1	0.42
E	Al Cru	12	13.5	6.6	11	6.6	11	6.3	10.3	0.51
F	SX Aur	11	12.5	6.6	11	6.6	11	5.6	10.3	0.54
G	V356 Sgr	10	11	—	—	7.8	13	4.7	12.1	0.68
H	V Pup	15	15	9.6	16	9.6	16	7.7	14.9	0.73

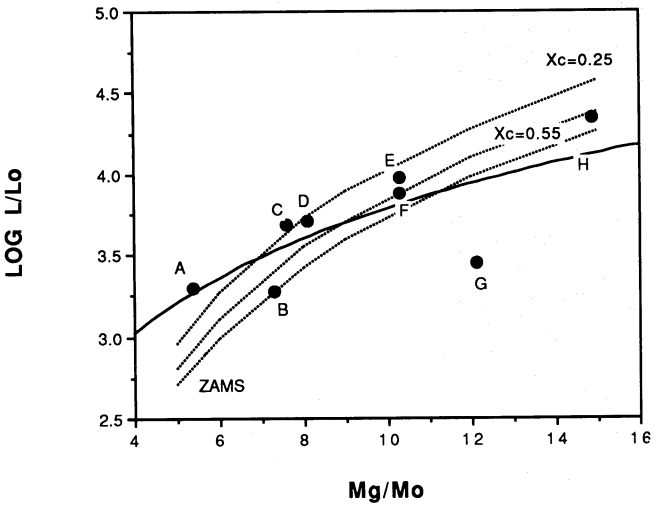

Fig. 5. Mass–luminosity diagram of the mass-gaining components of Table 3 (the full curve shows a best fit over the whole mass range). The dotted curves show the position of single star models with central hydrogen content $X_c = 0.7$ (Zero Age Main Sequence, ZAMS), $X_c = 0.55$ and $X_c = 0.25$

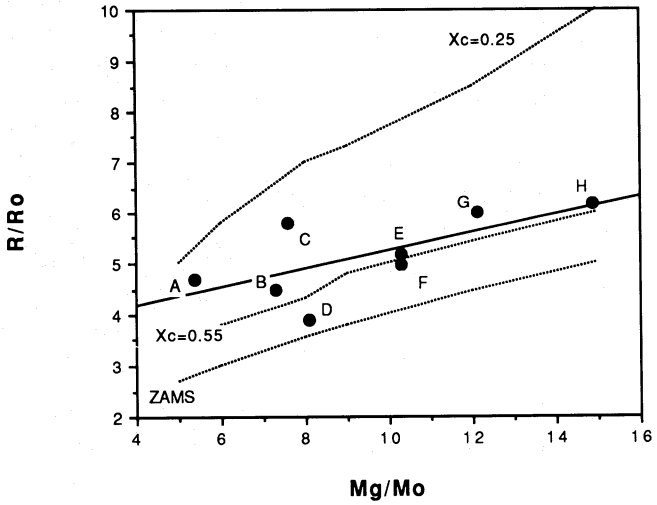

Fig. 6. The same as Fig. 5, but for the mass-radius relation

whole range of actual mass ratios between 1.4 and 5 is covered by the results from both initial mass ratios). We therefore checked possible deviations between the observed gainers and models of single stars for these central hydrogen abundances.

Figure 5 shows the luminosity of the gainers and the values for normal main sequence stars with central hydrogen equal to 0.25 (comparable to secondaries in systems with high initial mass ratio ~ 0.9), 0.55 (lower initial mass ratio, ~ 0.6), and for Zero Age Main Sequence stars (ZAMS). Figure 6 shows the corresponding radii. From the figures three conclusions can be drawn:

(1) According to the radii, the observed gainers are mostly at an early stage of core hydrogen burning, indicating an initial mass ratio well below 0.9.

(2) One gainer, V356 Sgr (system G), has a luminosity below the ZAMS value. But Wilson & Caldwell (1978) presented a model for this system with an opaque disk around the gainer in order to explain many of the peculiar features of this system.In addition, they suggested that if the spectral type of the gainer were B1 rather than B3 (that is, within a moderate range of uncertainty) then the current anomalous position of the gainer would be entirely resolved. Polidan (1989) argues well, from Voyager 2 ultraviolet observations, for an increase in the effective temperature for the hot star to 26 180 K (log $T_{eff} = 4.418$). This change would affect the light-curve solution in that the temperature of the cooler subgiant, T(s), would need to change too. But T(s) is constrained by the well-known spectral type, and

© European Southern Observatory • Provided by the NASA Astrophysics Data System

1994A&A...283..144F

the difference could be taken up in changing the properties of the inferred circumstellar disk around the hot star. So if the radii and masses remain unchanged, as one would expect, then this change in the temperature of the hot star would resolve the problem entirely. Further spectroscopic observations would be helpful.

The luminosity of the gainer of DM Per (B) is precisely on the ZAMS curve, disagreeing with the radius position.

(3) Practically all the mass gaining components show a discrepancy between the luminosity position and the radius position within the main sequence band: The gainers of V356 Sgr (G) and DM Per (B) are underluminous, all the others are overluminous. The gainer of DM Per is mildly underluminous, but only by 1 sigma, whilst that of V356 Sgr requires revision, as noted above. V Pup (H) is slightly underluminous with respect to the mass-radius relation, but can be considered as alright. The only other system for which luminosity and radius are in agreement is SX Aur (F).

The foregoing comparison was to models of single main sequence stars. From that we derived anomalies between observed individual components and normal stars (essentially explainable as uncertainties in the observations), and a general idea about the value of the initial mass ratio. As a preference for $q_i = 0.6$ emerges, we compared as a next step the luminosities and radii of the observed gainers with evolutionary tracks of mass accreting stars for $q_i = 0.6$ and masses $M_{li} = 5$–$15 M_\odot$, to derive an estimate of the initial mass. The results are given in Table 3. The table also gives the initial masses of the loser that are linked to the result of the gainer. First we note the agreement between the values obtained with the radius and those obtained with the luminosity, in spite of the discrepancies found above (cf. remark 3). Second, in Figs. 7 and 8 we plot the observed locations of the gainers in the M–L plane together with evolution

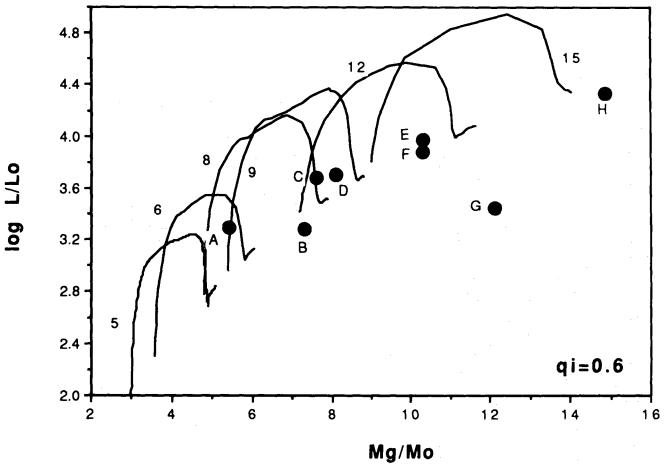

Fig. 7. Evolutionary tracks in the mass-luminosity diagram, of mass accreting components of buinary systems with initial primary masses $M_{li} = 5$, 6, 8, 12 and $15 M_\odot$ (indicated at the tracks) and mass ratio $q_i = 0.6$. The positions of the observed gainers of the systems of Table 3 are also shown

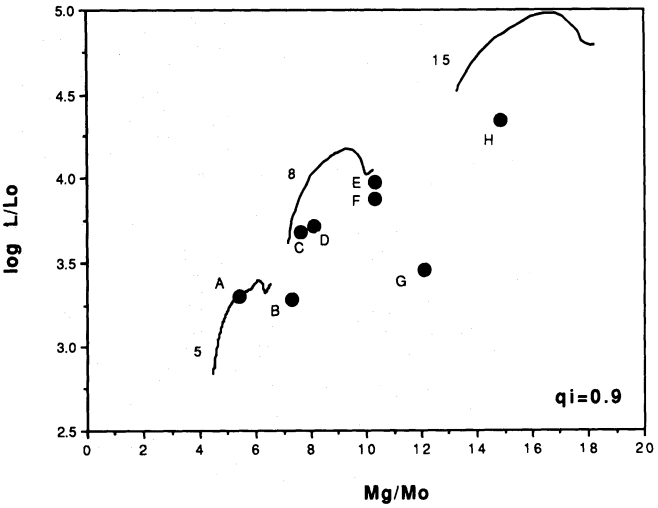

Fig. 8. The same as Fig. 7, but for $q_i = 0.9$ and only for gainers of systems with primary masses $M_{li} = 5$, 8 and $15 M_\odot$

tracks for the gainers with initial mass ratios of $q_i = 0.6$ and 0.9 respectively. In Fig. 7 ($q_i = 0.6$) the observed gainers are found to have good agreement with the evolution tracks, and be in the slow phase of mass accretion. But in Fig. 8 ($q_i = 0.9$) most of the observed gainers are found to lie below the evolution tracks, in systematic disagreement with the models. This confirms the tendency that was found in the comparison with single star models: the location of the gainers in the slow phase of mass exchange is in good agreement with that of the losers provided the initial mass ratio is of order 0.6 rather than 0.9.

Third, we find that the initial masses of the losers that are linked to the gainers (columns marked M_{li}/M_o L-curve, resp. M_{li}/M_o R-curve) are generally somewhat lower than the values obtained directly through the mass-luminosity positions (cf. Fig. 4). Again, except for TT Aur and AI Cru, these differences are small. Three systems deserve a remark.

Z Vul: The large luminosity and large radius of the gainer require a larger initial mass ratio, with a lower initial mass value for the loser.

DM Per: A better fit to its ZAMS position is obtained for a lower initial mass ratio. The corresponding mass M_{li} is then $6 M_\odot$.

V Pup: The ZAMS position requires also a lower mass ratio, and hence a larger mass M_{li}.

Adopting the values of M_{li} in column 4 (for $q_i = 0.6$, cf. Fig. 4) and those for M_{gi} in column 7 ($q_i = 0.6$, R-curves), we can calculate the mass transferred and the mass accreted. The ratio of the latter to the former gives ß, the fraction of mass accreted by the bright component (last column in Table 3). The values range between 0.38 (Z Vul) and 0.73 (V Pup).

© European Southern Observatory • Provided by the NASA Astrophysics Data System

1994A&A...283..144F

5. Contact systems

The table of HB87 also lists a number of contact systems. Their characteristics are given in Table 4. We extended this list with four other systems taken from the excellent compilation of Packet (1988, unfortunately never published in a journal): UW CMa (Leung & Schneider 1978), SV Cen (Drechsel et al. 1982), BH Cen (Leung et al. 1984) and RY Sct (Milano et al. 1981). We compare the contact systems both with main sequence models and with contact models from close binary calculations. However, the comparison must be regarded with caution (therefore it is restricted to the simple establishment of the results), for the following reasons:

(a) The parameters of these systems are not well known because of insufficient data of adequate quality, and often their contact nature is still uncertain. The spectra of these systems are difficult to study because they display few lines, and rotational broadening of the lines is high. Many systems are viewed at quite low inclinations, so that eclipses are partial and the determination of the mass ratio and the orbital inclination are not easily separated. The spectroscopic solution for BH Cen is still lacking, and there is still some doubt about the contact nature of SV Cen (Mochnacki 1985), in spite of the numerous confirmations. For UW CMa, the mass ratio given by Leung and Schneider is still uncertain (and hence the absolute dimensions). Even V348 Car needs higher resolution spectra (Hilditch & Evans 1985) to have more certainty about the mass ratio, in spite of the complete analysis of this system from these authors. The similar system AO Cas has also posed problems in terms of the determination of the mass ratio. But recent high-resolution spectral studies at optical (Gies & Wiggs 1991) and ultraviolet wavelengths (Stickland & Lloyd 1988; Bagnuolo & Gies 1991) have served to improve significantly the determination of the mass ratio of AO Cas, as well as the spectral types and assigned effective temperatures of both components. The revised masses and other parameters from Gies & Wiggs (1991) are given in Table 4.

(b) The dimensional characteristics of the models of the mass gaining components during contact are very sensitive to the accretion rate. This rate depends on the amount of mass loss from the system (50% for the present models) and on the absolute value of the rate. Slight changes in the value of the accretion rate lead to severe changes in the radius of the star (Kippenhahn et al. 1980).

(c) As mentioned by HB87, these systems are probably in the slow phase of a case A of mass transfer, exchanging mass while both components are still on the main sequence.

Figures 9 and 10 show the location of primary and secondary components in the mass-luminosity and mass-radius diagram resp., together with the contact parts of the evolutionary tracks for both components from the computations. Only systems with $q_i = 0.6$ and M_{1i} smaller than $30M_\odot$ show a contact phase, resulting in $\sim 20M_\odot$ as the largest mass value among the theoretical contact models. For the luminosity, the location of the observed stars falls more or less in the band occupied by the calculations. However, from Fig. 10 it is clear that the radii of the theoretical models are systematically too large compared to the observed ones. Compared to the position of the main sequence band we also note the difference in location between the luminosity and the radius. According to these figures, several contact components are located outside the theoretical main sequence band (below and above). Again, the dimensions depend largely on the precise value of the mass ratio, but also on the possible contribution of gas streams and circumbinary matter (e.g. AO Cas and SV Cen).

Table 4. Characteristics of contact systems. For mass, radius, luminosity, solar units are used. The columns with E give the error on the preceding value, similar as in Table 1. The first part gives the systems in the table of HB87 (see references in that paper), the second part shows the data (without error estimates) of four additional systems appearing in the compilation of Packet (1988). References are given in the text

System	Comp.	Period	log M	$E(M)$	log R	$E(R)$	log T	$E(T)$	log L	$E(L)$
V348 Car	p	5.562	1.544	0.012	1.312	0.013	4.476	0.019	5.480	0.080
B1 + B	s		1.544	0.012	1.312	0.013	4.418	0.017	5.250	0.070
Y Aur	p	4.025	1.500	0.044	1.215	0.053	4.514	0.023	5.430	0.150
O9.2 + O9.4	s		1.322	0.097	1.127	0.052	4.486	0.023	5.160	0.150
V382 Cyg	p	1.886	1.430	0.044	0.964	0.033	4.575	0.015	5.170	0.090
O7.3 + O7.7	s		1.279	0.043	0.875	0.029	4.565	0.015	4.650	0.080
AO Cas	p	3.523	1.093	0.056	1.013	0.032	1.519	0.019	5.060	0.070
O8.5 + O8.5	s		1.262	0.041	0.898	0.111	4.519	0.019	4.820	0.260
TU Mus	p	1.387	1.371	0.046	0.903	0.022	4.555	0.015	4.900	0.080
O7.8 + O8.2	s		1.199	0.041	0.820	0.020	4.545	0.015	4.720	0.070
V701 Sco	p	0.762	1.013	0.025	0.633	0.008	4.371	0.019	3.707	0.076
B1+	s		1.013	0.025	0.631	0.008	4.367	0.019	3.688	0.076
RZ Pyx	p	0.656	0.760	0.026	0.430	0.016	4.230	0.025	2.737	0.107
B5 +	s		0.675	0.026	0.400	0.010	4.255	0.026	2.656	0.106

© European Southern Observatory • Provided by the NASA Astrophysics Data System

1994A&A...283..144F

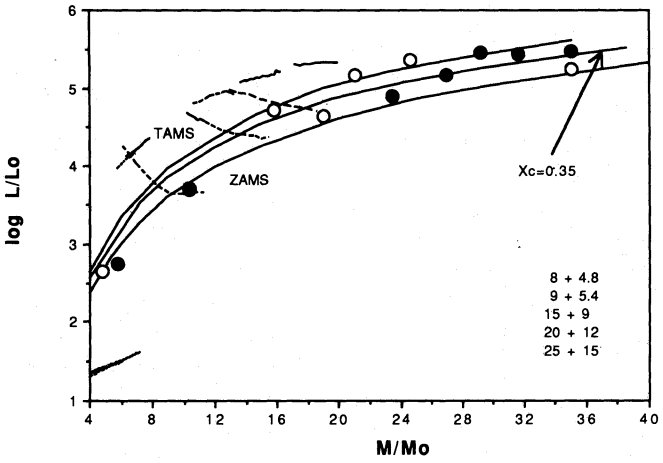

Fig. 9. Position in the mass–luminosity diagram of the components of the contact systems of Table 4 (black dots: bright components; open circles: less bright secondaries). The large curves show the Zero Age Main Sequence (ZAMS), the Terminal Age Main Sequence (TAMS), and the line of single star models with $X_c = 0.35$. The short curves show the contact part of the evolutionary tracks for different systems (initial masses are shown at lower right)

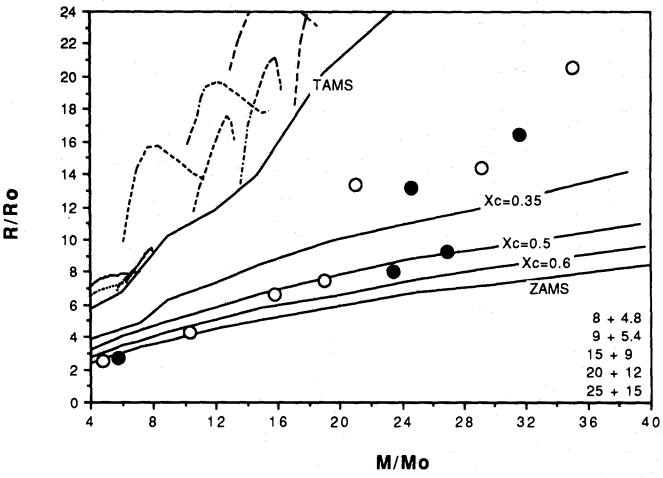

Fig. 10. The same as Fig. 9 for the mass-radius relation, but in this figure we added lines of single star models with X_c = 0.5 and 0.6

Taking the lines of equal central hydrogen content as guidelines, the systems of Fig. 10 fall into two groups, one with X_c less than 0.35 (V348 Car, LY Aur, AO Cas), and one with X_c between 0.5 and 0.7. In the mass-luminosity diagram the less massive component of TU Mus shifts from the second to the first group, with a position that reflects more a value of $X_c \sim 0$.

We explored the possibility of a case A mass transfer process, suggested by HB87, in somewhat more detail. Is it possible that the observed period is the result of a rapid decrease from a much larger initial period, through mass and angular momentum loss from the system? To investigate this, we looked for estimates of the initial masses and period, for a given value of $\beta = \Delta M(\text{gainer})/\Delta M(\text{loser})$, given q_i and the present masses $M_{g,obs}$ and $M_{l,obs}$. Values of $\beta = 1$, 0.5 and 0 were adopted. In that case the mass lost by the loser is derived as

$$\Delta M(\text{loser}) = (M_{g,obs} - q_i \times M_{l,obs})/(q_i + \beta).$$

The initial masses can then be determined in a straightforward manner. For the angular momentum loss we applied the algorithm given by Vrancken et al. (1991) (see also Yungelson & Tutukov 1991), with values of 2, 4 and 7 for the parameter g.

Specifically, we determined the conditions for $q_i = 1$, $q_i = 0.75$ and $q_i = 0.5$, taking the smaller component as the loser. Both for the conservative ($\beta = 1$) as for the nonconservative ($\beta < 1$) cases of mass transfer, we find for all systems that the critical Roche radius at the onset of the mass transfer is always smaller than the maximum radius of the primary at the end of the main sequence; that is, mass exchange must proceed as in case A. The only way to avoid this is to assume very low initial mass ratios of the order of 0.4 or less. Alternatively, adopting the presently more massive component as the loser results in similar or even lower values for the critical radius.

As an example we show the results for the system with the largest period in the sample, RY Sct, in Fig. 11. The smaller the initial mass ratio, the larger M_{li} becomes. For large masses the maximum radius on the main sequence is roughly equal to M_{li}, whereas the critical Roche radius is between 1/2 and 2/3 of it. This clearly shows that a case A is unavoidable.

6. Discussion and conclusions

Although a number of components in detached systems show a difference with theoretical models that is larger than 15%, the majority agrees well with them. We find good correspondence between theoretical and observed characteristics for stars with masses between $4.5 M_\odot$ and $17 M_\odot$.

As for the semidetached systems, an initial mass ratio of around 0.6 seems to be preferred to the larger value of 0.9. Even with this value all systems evolve in a nonconservative way (with β ranging between 0.4 and 0.7). Because of their short periods some of them may well evolve according to case A. However, because of the mass and angular momentum loss from the system, a decision between case A or B cannot be made in the present general approach.

If we compare the semidetached systems having the same (or nearly the same) initial primary mass, we find the same value of β for the systems TT Aur and SX Aur, $\beta = 0.54$. As the periods are rather short but comparable (resp. 1.33 d and 1.21 d), the calculation of a restricted grid of case A models, together with improved observations (especially for TT Aur) would offer an interesting opportunity of studying two systems coming from the same parent system. The same holds for Z Vul and DM Per, but for these

© European Southern Observatory • Provided by the NASA Astrophysics Data System

1994A&A...283..144F

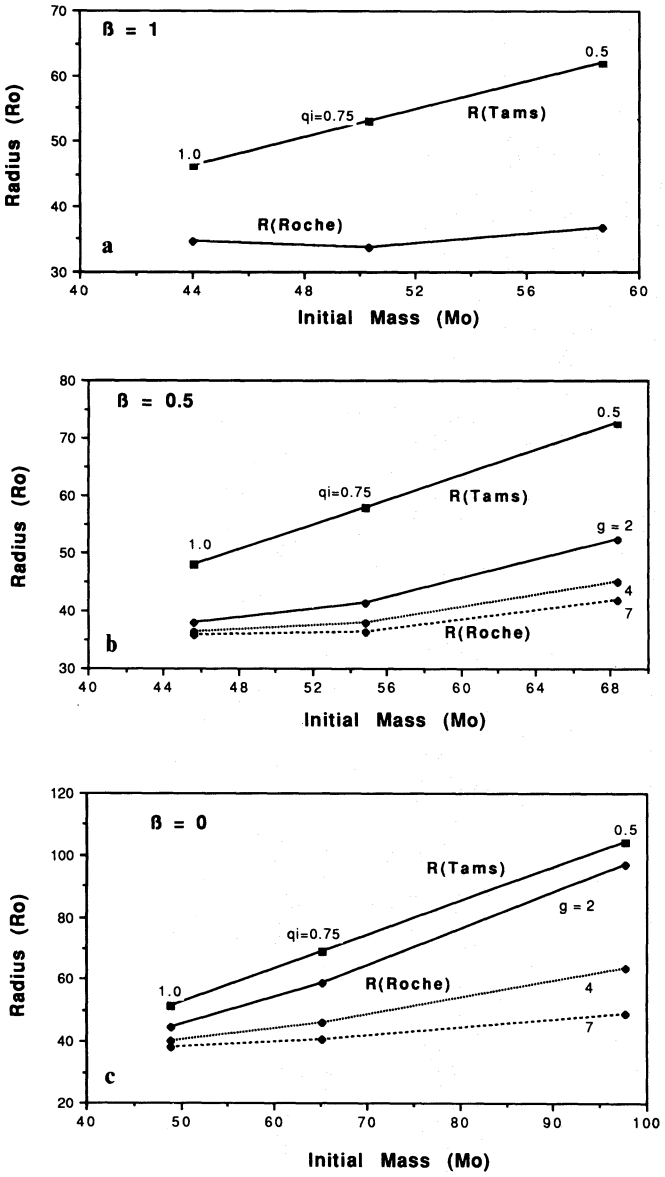

Fig. 11a–c. Radius at Terminal Age Main Sequence, R (TAMS: squares) and Roche radius, R (Roche: diamonds), prior to mass transfer for the less massive star of the system RY Sct, as a function of the initial mass, for three values of the initial mass ratio (q_i = 1.0, 0.75, 0.50). **a** shows the results for the conservative case (ß = 1), **b** for the case ß=0.5 and three cases of angular momentum loss (indicated by $g = 2, 4$ and 7), **c** for the case of no accretion (ß = 0) and the same angular momentum losses

two systems the fraction of transferred mass differs severely (ß = 0.38 and 0.64 resp.). But also this offers an opportunity to test nonconservative models, again given accurate observations are available.

The radii of the theoretical models of the contact systems are systematically too large compared to the observed ones. However the observed systems all seem to evolve according to the case A of mass transfer, and in that case the corresponding models will not show such a large radius increase as in the theoretical case B models. For a more meaningful comparison an appropriate set of case A computations is needed.

With regard to future observational work on the most massive systems, it is clear that the use of procedures for the tomographic separation of spectra (Bagnuolo & Gies 1991) will have substantial impact on improving the determination of fundamental parameters (see, e.g. Hill et al. 1993, on CC Cas). These procedures ensure not only improved quality of spectra for radial-velocity and line profile studies, but also reveal the existence of circumstellar matter and colliding winds. But, as is often the case, more high-precision photometry is required also to secure accurate and complete light curves for analysis. With orbital periods necessarily in the region of days to tens of days for most OB systems, the determination of such accurate light curves is not a trivial matter.

Acknowledgements. This research was financed by grant S2/5 E96 (National Fund of Scientific Research of Belgium) and by grant BD/346/90-RM from JNICT, Portugal. The authors thank the referee for the critical yet constructive comments.

References

Andersen J., 1975, A&A 44, 355
Andersen J., 1991, A&AR 3, 91
Andersen J., Clausen J.V., 1983, A&A 213, 183
Bagnuolo W.G., Gies D.R., 1991, ApJ 376, 266
Bell S.A., Hilditch R.W., Adamson A.J., 1986, MNRAS 223, 513
Bell S.A., Hilditch R.W., Adamson A.J., 1987, MNRAS 224, 649
Benson R.S., 1970, Ph.D. Thesis, Univ. of California, Berkeley
Broccato B., Castellani V., 1991 (preprint)
Clausen J.V., Gimenez A., 1991, A&A 241, 98
De Greve J.P., 1993, A&AS 97, 527
De Greve J.P., 1986, Space Sci. Rev. 43, 139
De Greve J.P., de Loore C., 1992, A&AS 96, 653
de Loore C., De Greve J.P., 1992, A&AS 94, 453
Drechsel H., Rahe J., Wargau W., Wolf B., 1982, A&A 110, 246
Flannery B.P., Ulrich R.K., 1977, ApJ 212, 533
Gies D.R., Wiggs M.S., 1991, ApJ 375, 321
Hilditch R.W., 1973, MNRAS 164, 10
Hilditch R.W., Bell S.A., 1987, MNRAS 229, 529 (HB87)
Hilditch R.W., Evans T., 1985, MNRAS 213, 75
Hilditch R.W., Hill G., Khalesseh B., 1992, MNRAS 254, 82
Hill G., Batten A.H., 1984, A&A 141, 39
Hill G., Hilditch R.W., Aikman G.C.L., Khalesseh B., 1993, A&A (submitted)
Holmgren D.E., Hill G., 1991, A&A 248, 129
Holmgren D.E., Hill G., Fisher W.A., 1990a, A&A 236, 409
Holmgren D.E., Hill G., Fisher W.A., Scarfe C.D., 1990b, A&A 231, 89
Kippenhahn R., Meyer-Hofmeister E., 1977, A&A 54, 539
Kippenhahn R., Ruschenplatt G., Thomas H.-C., 1980, A&A 91, 175
Kippenhahn R., Weigert A., 1966, Mitt. Astron. Ges. 21, 106

© European Southern Observatory • Provided by the NASA Astrophysics Data System

1994A&A...283..144F

Leung K.-C., Schneider D.P., 1978, ApJ 222, 924
Leung K.-C., Sistero R.F., Zhai D.-S., Grieco A., Candellero B., 1984, AJ 89, 872
Maeder A., Meynet G., 1987, A&A 182, 243
Milano L., Vittone A., Ciatti F., Mammano A., Margoni R., Strazzulla G., 1981, A&A 100, 59
Mochnacki S.W., 1985, in: Eggleton P.P., Pringle J.E. (eds.) Interacting Binaries. Reidel, Dordrecht, NATO ASI Ser. C, Vol. 150, p. 51
Packet W., 1988, Ph.D. Thesis, V.U.B., Brussels
Packet W., De Greve J.P., 1979, A&A 75, 255
Polidan R.S., 1989, Space Sci. Rev. 50, 85
Popper D.M., 1980, ARA&A 18, 115
Popper D.M., Hill G., 1991, AJ 101, 600
Rogers F.J., Iglesias C.A., 1992, A&AS 96, 269
Schaller G., Schaerer D., Meynet G., Maeder A., 1992, A&AS 96, 269
Shobbrook R.R., Herbisan-Evans D., Johnston I.D., Lamb N.R., 1969, MNRAS 145, 131
Stickland D.J., Lloyd C., 1988, Observatory 108, 174
Vrancken M., De Greve J.P., Yungelson L., Tutukov A., 1991, A&A 249, 411
Wachmann A.A., Popper D.M., Clausen J.V., 1986, A&A 162, 62
Wilson R.E., Caldwell C.N., 1978, ApJ 221, 917
Yungelson L., Tutukov A., 1991, in : van der Hucht K., Hidayat B. (eds.) Wolf-Rayet Stars and Interrelations with Other Massive Stars in Galaxies. Kluwer, Dordrecht, p. 459
Zahn J.-P., 1991, A&A 252, 179

© European Southern Observatory • Provided by the NASA Astrophysics Data System